

The test results of the Silicon Tungsten Tracker of DAMPE

V. Gallo^{*1}, G. Ambrosi², R. Asfandiyarov¹, P. Azzarello¹, P. Bernardini^{3,4}, B. Bertucci^{2,5}, A. Bolognini^{2,5}, F. Cadoux¹, M. Caprai², I. De Mitri^{3,4}, M. Domenjoz¹, Y. Dong⁶, M. Duranti^{2,5}, R. Fan⁶, P. Fusco^{7,8}, F. Gargano⁷, K. Gong⁶, D. Guo⁶, C. Husi¹, M. Ionica^{2,5}, D. La Marra¹, F. Loparco^{7,8}, G. Marsella^{3,4}, M.N. Mazziotta⁷, A. Nardinocchi^{2,5}, L. Nicola¹, G. Pelleriti¹, W. Peng⁶, M. Pohl¹, V. Postolache², R. Qiao⁶, A. Surdo⁴, A. Tykhonov¹, S. Vitillo¹, H. Wang⁶, M. Weber¹, D. Wu⁶, X. Wu¹, F. Zhang⁶

¹*Département de Physique Nucléaire et Corpusculaire, University of Geneva, Geneva, Switzerland*

²*Istituto Nazionale di Fisica Nucleare Sezione di Perugia, Perugia, Italy*

³*Dipartimento di Matematica e Fisica "E. De Giorgi", Univerisità del Salento, Lecce, Italy*

⁴*Istituto Nazionale di Fisica Nucleare Sezione di Lecce, Lecce, Italy*

⁵*Dipartimento di Fisica e Geologia, Univerisità di Perugia, Perugia, Italy*

⁶*Institute of High Energy Physics, Chinese Academy of Sciences, Beijing, China*

⁷*Istituto Nazionale di Fisica Nucleare Sezione di Bari, Bari, Italy*

⁸*Dipartimento di Fisica "M.Merlin" dell'Univerisità e del Politecnico di Bari, Bari, Italy*

E-mail: Valentina.Gallo@unige.ch

The DAMPE (DARK Matter Particle Explorer) is one of the five satellite missions in the framework of the Strategic Pioneer Research Program in Space Science of the Chinese Academy of Science (CAS). DAMPE is a powerful space telescope which has as main scientific objective the identification of possible Dark Matter signatures thanks to the capability to detect electrons and photons in a wide range of energy from 5 GeV up to 10 TeV and with unprecedented energy resolution. Moreover, the DAMPE satellite will contribute to a better understanding of the origin and propagation mechanisms of high energy cosmic rays thanks to the measurement of the flux of nuclei up to 100 TeV. Hints in the sector of high energy gamma astronomy are also expected thanks to its excellent photon detection capability.

In this document we will present a detailed description of the DAMPE tracker: the silicon-tungsten tracker-converter (STK). The STK is being developed by an international collaboration composed of groups from University of Geneva, INFN Perugia, INFN Bari, INFN Lecce and Institute of High Energy Physics, Beijing. The STK is made of 192 ladders, each of them is made up of four single-sided silicon strip detectors. In the following, the ladder performances in terms of charge collection and spatial resolution evaluated during a test beam period at the CERN SPS (Super Proton Synchrotron) in May 2015 are presented.

*The 34th International Cosmic Ray Conference,
30 July- 6 August, 2015
The Hague, The Netherlands*

*Speaker.

1. Introduction

The DAMPE detector [1] is made up, as shown in Fig. 1, of the following sub-detectors: a double layer of plastic scintillator strips detector (PSD) that serves as anti-coincidence, followed by silicon- tungsten tracker-converter (STK), a Bismuth Germanium Oxide (BGO) imaging calorimeter and a neutron detector (NUD).

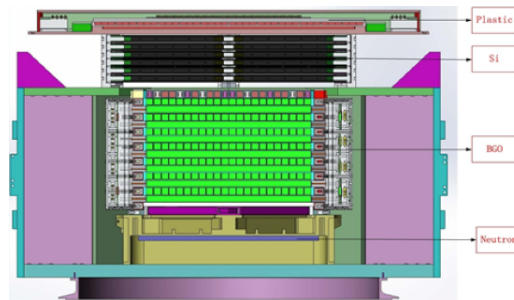


Figure 1: Layout of the DAMPE detector.

The PSD covers an area of $82 \times 82 \text{ cm}^2$ and is made of one double layer (one for the X and one for the Y direction) of scintillating strips detector. The scintillating strips are 1 cm thick, 2.8 cm wide and 82 cm long and are staggered by 0.8 cm in each layer for a fully area coverage. The PSD has a position resolution of 6 mm and a charge resolution of 0.25 for nuclei with an atomic number Z going up to 20.

The PSD is followed by the silicon tracker detector. The STK is made of 6 tracking double layers of single sided silicon strip detectors, a more detailed description is reported section 2.

The core of the DAMPE satellite is the imaging calorimeter that is placed just after the STK. The calorimeter is made of 14 layers of BGO bars of $2.5 \times 2.5 \text{ cm}^2$ in cross section and 60 cm in length, making it the longest BGO crystals ever produced. The bars are placed in a hodoscopic arrangement and read out at both ends by photomultipliers. The total thickness of the calorimeter is equivalent to 31 radiation lengths and 1.6 interaction lengths making it the deepest calorimeter ever used in space. The expected electromagnetic energy resolution is of 1.5% above 100 GeV, and a very good hadronic energy resolution of better than 40% above 800 GeV is also foreseen.

Finally, in order to detect delayed neutron resulting from hadron shower and to improve the electron/proton separation power a neutron detector is placed just below the calorimeter. The NUD consists of 16, 1 cm thick, boron-doped plastic scintillator plates of $19.5 \times 19.5 \text{ cm}^2$ large, each read out by a photomultiplier.

The DAMPE satellite has been successfully constructed and it is at the end of its qualification phase. The launch is foreseen for December 2015.

In the following, after a more complete description of the STK, the performances of its constituents, the single sided silicon detectors, in terms of charge collection and spatial resolution are presented. The results have been obtained during a test beam period at CERN Super Proton Synchrotron (SPS) [2] in May 2015.

2. The silicon-tungsten tracker-converter.

The silicon-tungsten tracker-converter [3] has been designed to measure charged particle tracks, to convert incoming photons into electron-positron pairs in order to measure the photon direction, and to measure the charge of cosmic rays.

The STK consists of a total of 7 planes forming 6 tracking double layers. Each tracking layer is equipped with single-sided silicon strip detectors placed to measure the two orthogonal views perpendicular to the pointing direction of the apparatus. In order to allow photon conversion, three layers of tungsten plates with thickness of 1 mm are inserted into the support trays of the second, third and fourth tracker plane.

Each tracking layer is made of 16 ladders each formed of 4 single-sided AC-coupled silicon micro-strip detectors for a total of 192 ladders. The sensors have been built by Hamamatsu Photonics [4] and are $320\ \mu\text{m}$ thick, $9.5 \times 9.5\ \text{cm}^2$ in size, and segmented into 768 strips with a $121\ \mu\text{m}$ pitch. In order to limit the number of readout channels and keep a good performance in terms of space resolution the readout is done only every other strip for a total of 384 channels per ladder that are read by 6 VA140 ASIC chips. Since the analogue readout is used and thanks to the charge division on the floating strips, even if not all the strips are readout the position resolution is expected to be better than $80\ \mu\text{m}$ for most incident angles, as discussed in section 3.3. The full tracker uses 768 sensors corresponding to a total silicon area of $7\ \text{m}^2$, comparable to the silicon area of the AMS-02 tracker [5].

The STK has been successfully build in spring 2015. A picture of the tracker before the assembly of the last tray, the front-end electronics and the cooling and supporting structures is shown in Fig. 2. In the picture the sixteen ladders forming one sensitive layer of the STK are clearly visible.

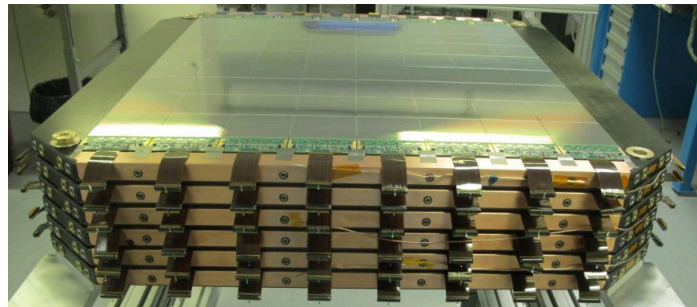


Figure 2: Picture of the silicon-tungsten tracker-converter before the assembly of the last tray, of the DAQ electronics and the cooling and supporting structures. The total silicon area is of about $7\ \text{m}^2$.

3. The STK silicon detectors performances.

Charge measurements are very important for space experiments due to the abundance ratios of secondary to primary particles, such as boron to carbon, that are excellent quantities to test cosmic ray propagation models. The first step to optimise these measurements is to have a complete knowledge of charge sharing and propagation processes among the silicon detectors.

In order to characterise the main properties of the ladders composing the STK, two ladders have been carefully studied using 400 GeV protons. The ladders were installed in the middle of a beam telescope made of 6 HV-CMOS pixel detectors [6] and capable to provide a track resolution of about $5 \mu\text{m}$. The performances in terms of charge collection and of spatial resolution for different proton beam angles of incidence have been studied. Since the results for both ladders are very similar, in the following we will focus on only one.

3.1 Data reconstruction

The digitised value of each ladder channel i in the event j defined as ADC_{ij} is made of the sum of the following contributions:

$$ADC_{ij} = ped_i + cn_j + noise_{ij} + signal_{ij} \quad (3.1)$$

In Eq. 3.1, the *noise* is the random component of the sampled value, while *ped* and *cn* correspond to the pedestal and the common noise defined, respectively, as:

$$ped_i = \frac{1}{N} \sum_{j=0}^N ADC_{ij}; \quad cn_j = \frac{1}{64} \sum_{i=0}^{64} (ADC_{ij} - ped_i)$$

Pedestals are calculated averaging on $N(=1024)$ events, while the common noise is computed event by event on 64 channels, i.e. on a chip by chip basis. Once the common noise is evaluated, the σ value, i.e. the intrinsic noise of each channel can be defined as:

$$\sigma_i = \sqrt{\frac{1}{N} \sum_{j=0}^N (ADC_{ij} - ped_i - cn_j)^2}$$

This value results to be of about 3 ADC as shown on the left side of Fig. 3.

The charge produced by a particle crossing the silicon detector is reconstructed with a cluster algorithm using a high threshold of $4 \times \sigma$ for the seed strip and a low threshold of $1.5 \times \sigma$ for the neighbour strips. The high threshold, as shown on the right side of Fig 3, has been chosen to maximise the signal selection and minimise the noise contribution.

3.2 Performance

The typical cluster charge distribution in terms of ADC of particle hitting perpendicularly the ladder is shown on the left side of Fig. 4. The two peaks shape of the cluster charge distribution is due to the charge sharing among the strips and the impact position of the particle. When the particle hits the floating strip, about 70% of the charge is recovered by the two neighbour readout strips, while when the readout strip is hit all the charge is collected by one single strip resulting in higher charge collection. In case of inclined particles, the charge will be shared among more strips with a consequent increase of the cluster size, as shown in the right side of Fig. 4. As a result, even for very inclined particles (note that an angle of incidence of 60° corresponds to the geometrical acceptance of STK that is limited by the calorimeter) the number of strips composing the cluster is limited to a few strips. This allows to have a limited data size, important for transfer of the data at ground.

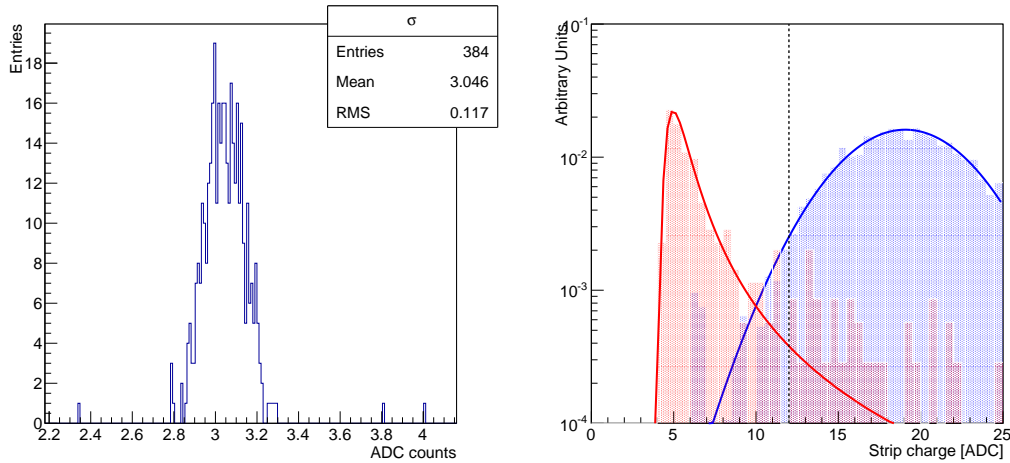


Figure 3: (Left) Intrinsic noise of the ladders. (Right) The noise contribution is described by the red area while the signal is the blue area. The black line indicates the high threshold cut of $4 \times \sigma$ chosen for the cluster algorithm.

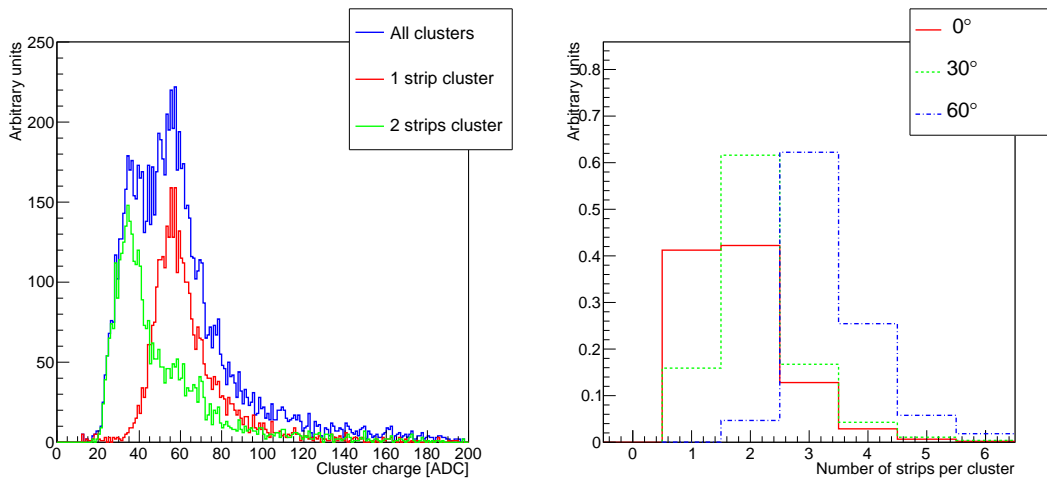


Figure 4: (Left) Energy distribution in terms of ADC of particles hitting perpendicularly (angle of incidence of 0°) the ladder. (Right) Distribution of the number of strips per cluster at different angles of incidence.

Thanks to the high resolution ($5 \mu\text{m}$) of the beam telescope used to reconstruct the track, a detailed study of the behaviour of the ladder charge collection could be carried on for several particle angles of incidence. Defining 0° as the angle orthogonal to the ladder, data within a range from 0° to 70° with 10° step have been collected. In the following, the results for three representative angles of incidence of 0° , 30° and 60° are presented.

In Fig. 5, the cluster charge distributions for the three angles of incidence is shown together with the simulated cluster charge distribution obtained using a Geant4 [7] simulation implemented in the DAMPE Software Framework [8]. The sharing of the charge among the strips depends on

the particle angle of incidence and the two peaks shape of the cluster charge distribution becomes less present as the angle of incidence increases, i.e. as the charge is released among more strips of the silicon detector.

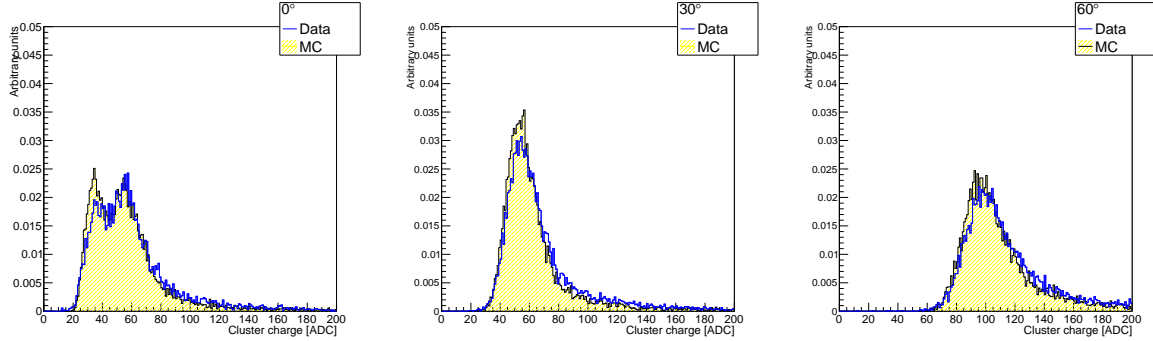


Figure 5: Cluster charge distribution in terms of ADC compared with Monte Carlo of particles hitting the ladder with an angle of incidence of: 0° (Left), 30° (Center) and 60° (Right).

The dependence of the collected charge with respect to the angle of incidence is also shown in Fig. 6, where the cluster charge is plotted in terms of the number of strips forming the cluster. If we consider, for example, clusters with two strips, the 30% loss of charge due to the charge sharing between two readout strips is partially recovered as the angle of incidence increases. Moreover,

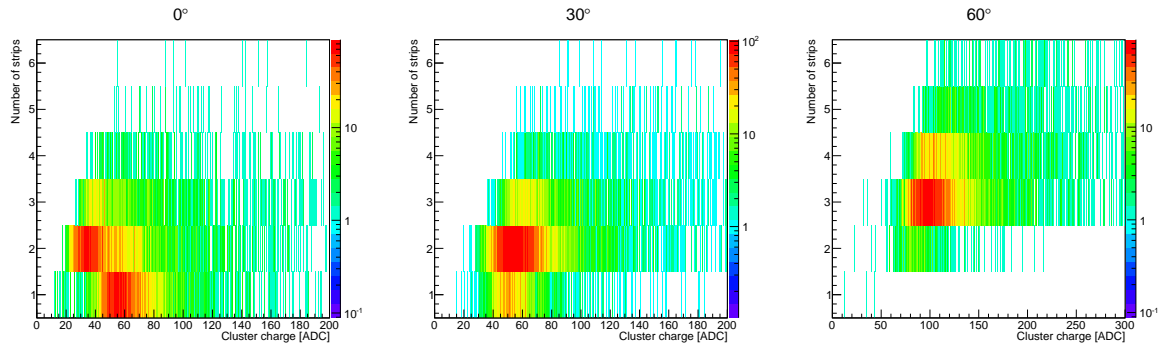


Figure 6: Cluster charge distribution in terms of ADC as a function of cluster size for particles hitting the ladder with an angle of incidence of: 0° (Left), 30° (Center) and 60° (Right).

since the readout is done only every other strip, the impact position of the incoming particles has to be taken into account. In Fig. 7 is shown the cluster charge as a function of the track impact position (IP) as estimated from the beam telescope.

As a consequence, the cluster charge has to be corrected for both the particle impact position and angle of incidence. These corrections will be very important for the study of heavy nuclei realising higher charge, as also seen in AMS-02 [9].

3.3 Spatial resolution

The spatial resolution of the STK silicon ladders has been also evaluated. Defining as impact

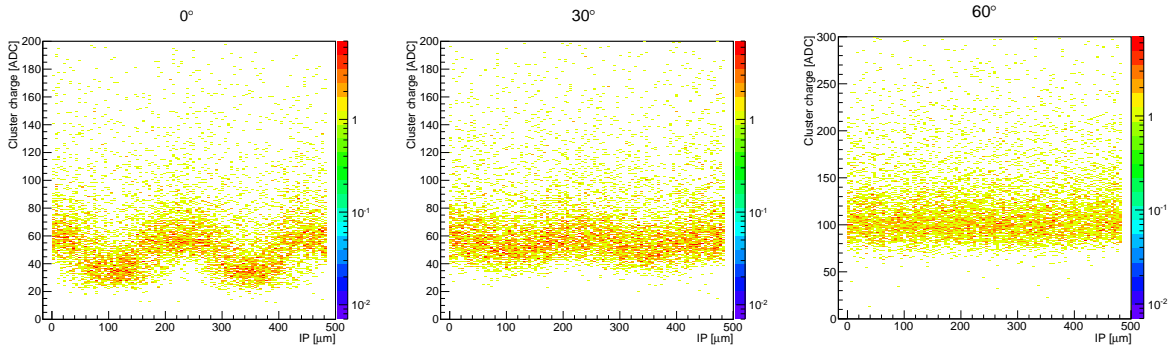


Figure 7: Cluster energy as a function of the reconstructed impact position (IP), i.e. within $500 \mu\text{m}$ three consecutive readout strips placed at 0, 242 and $484 \mu\text{m}$ are shown. The particle angles of incidence shown are: 0° (Left), 30° (Center) and 60° (Right).

point (IP) the position of the track on the silicon ladder as extrapolated by the beam telescope, the residual can be defined as: $residual = IP - cog$ where cog is the centre of gravity of the cluster obtained as weighted mean of the position of each strip. The residual distributions for the angles of incidence of 0° , 30° and 60° are shown in Fig 8 together with the Gaussian fit. Then, the resolution

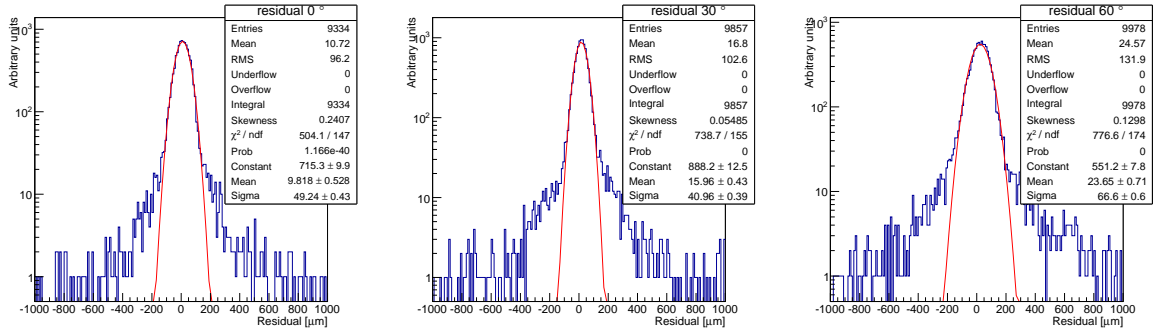


Figure 8: Residual: 0° (Left), 30° (Center) and 60° (Right) degrees. The resulting σ of the Gaussian fit represent the spatial resolution.

can be extrapolated by the σ of the Gaussian fit, note that the contribution due to the resolution of the beam telescope is negligible.

As a result, in Fig 9, the resolution for particle angles of incidence going from 0° to 70° in steps of 10° is shown. Thanks to the analogue readout used and to the charge division on floating strips, the spatial resolution results to be lower than $50 \mu\text{m}$ for an angle of incidence less than 40° and lower than $80 \mu\text{m}$ within the acceptance of the STK (60°).

4. Conclusion

The STK has been successfully completed in April 2015. The characterisation of its constituents, the silicon ladders, in terms of charge collection and spatial resolution has been reported.

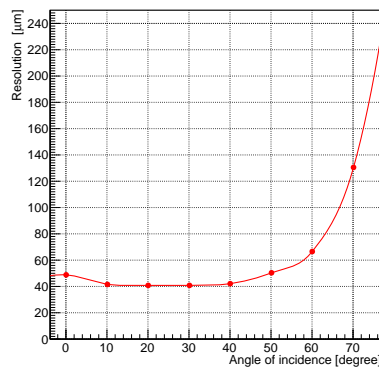


Figure 9: Spatial resolution as a function of particles angle of incidence. It results to be lower than $50 \mu\text{m}$ for an angle of incidence less than 40° and lower than $80 \mu\text{m}$ within the acceptance of the STK.

The charge collection has been studied in terms of impact point and angle of incidence of the incoming particle. These measurements will be of fundamental importance for the calibration of the full STK. Moreover, the test beam measurements confirm the importance of the choice of the analogue readout. Even if the readout is implemented only every other strip, a good resolution is achieved. Within the whole acceptance of the STK the ladder spatial resolution results to be well below $80 \mu\text{m}$ and lower than $50 \mu\text{m}$ for an angle of incidence less than 40° .

The DAMPE satellite has been successfully assembled in spring 2015 and its launch is foreseen for December 2015.

References

- [1] J. Chang, in *The 7th international workshop " the Dark Side of the Universe" (DSU) 2011*.
- [2] CERN Super Proton Synchrotron (SPS), <http://home.web.cern.ch/about/accelerators/super-proton-synchrotron>.
- [3] X. Wu et al., *The Silicon-Tungsten Tracker of the DAMPE Mission*, in proceeding of 34th ICRC, **1192** (2015).
- [4] HAMAMATSU, <http://www.hamamatsu.com/us/en/index.html>.
- [5] B. Alpat et al. , *The internal alignment and position resolution of the AMS-02 silicon tracker determined with cosmic-ray muon*, Nucl. Instrum. and Meth. A 613 (2010) 207-217.
- [6] B. Ristic et al., *Measurements on HV-CMOS active sensors after irradiation to HL-LHC fluences*, in proceeding of PIXEL 2014 , 2015 JINST 10 C04007.
- [7] S. Agostinelli et. al., *Geant4 a simulation toolkit*, Nucl. Instrum. Meth. A 506, 3 (2003) 250.
- [8] A. Tykhonov et al., *Software framework and the reconstruction software of the DAMPE gamma-ray mission*, in proceeding of 34th ICRC, **1193** (2015).
- [9] J. Alcazar et al. , *Charge determination of nuclei with the AMS-02 silicon tracker*, Nucl. Instrum. and Meth. A 540 (2005) 121.